ELSEVIER

Chemical Physics 207 (1996) 477–498

Chemical Physics

Proton-transfer reaction dynamics

Abderrazzak Douhal [a], Françoise Lahmani [b], Ahmed H. Zewail [c,*]

[a] *Departamento de Quimica Fisica, Facultad de Quimicas, Seccion de Toledo, Universidad de Castilla-La Mancha, San Lucas 3, 45002 Toledo, Spain*

[b] *Laboratoire de Photophysique Moleculaire, Bat. 213, Universite de Paris-sud, CNRS, 91405 Orsay, France*

[c] *Arthur Amos Noyes Laboratory of Chemical Physics, California Institute of Technology, Pasadena, CA 91125, USA*

Received 12 January 1996

Abstract

In this article we discuss the progress made in understanding intramolecular and intermolecular reactions of proton (or hydrogen-atom) transfer. Femtosecond real-time probing, together with spectroscopic studies, in molecular beams are presented with selected examples of reactions. Reaction rates, tunneling dynamics and the nature of the reaction coordinate are examined and related to two-state multidimensional potential energy surfaces.

1. Introduction

The transfer of a proton or a hydrogen atom from one group (OH, $-NH_2$) to another (C=O, –N=) has been referred to as 'the most general and important reaction in chemistry' [1]. This reaction is a cornerstone of many processes [2] including acid–base neutralization [3], and enzymatic reactions [4].

Depending on the system, the reaction can be intramolecular or intermolecular, and may occur by thermal and/or photoinduced activation, in a barrierless process or through a barrier (proton tunneling).

In organic bifunctional molecules which contain both hydrogen-atom donor and acceptor groups in close proximity, an intramolecular hydrogen bond (IHB) is generally formed in the electronic ground state. The intramolecular redistribution of electronic charge due to photon absorption in these kinds of molecules induces an elementary and fast reorganization of the molecular structure generally referred to as electronically excited-state intramolecular proton transfer (ESIPT). The most striking feature of the dynamics in these systems is the ultrafast nature of the ESIPT reaction ($k_{ESIPT} > 10^{12}$ s^{-1}), and for the spectroscopy the highly-Stokes-shifted fluorescence (6000–10000 cm^{-1}) of the product tautomer.

Aromatic molecules bearing an acidic proton such as phenol, $\alpha(\beta)$-naphthol, hydroxyleines, 7-hydroxycoumarins, and 7-azaindole are among the most investigated systems showing excited-state intermolecular proton-transfer. In this kind of process, the proton transfer occurs between the solute and the solvent, but in some cases it may occur in hydrogen bonded dimers. The H-bonded complex (AH...solvent, or AH...AH) is generally prepared in the ground state and its absorption spectrum is red shifted relative to that of the non-hydrogen bonded solute. The large Stokes shift (4000–8000 cm^{-1}) is a

* Corresponding author.

PII S0301-0104(96)00067-5

common signature of the occurrence of excited-state proton-transfer reaction.

This article mainly deals with the reaction dynamics. In Section 2, we will focus on the understanding of the process, and characterize the major features of the potential energy surface (PES) from experimental and theoretical views. We give a description of the reaction dynamics, first using the O–H bond as the reaction coordinate, and later the two-dimensional model using the O–H coordinate and the distance between the involved heteroatoms. Tunneling and non-radiative mechanisms are also discussed.

In Section 3, we consider in more detail three selected systems, methyl salicylate (MS), 1-hydroxy-2-acetonaphthone (HAN), and 2-(2′-hydroxyphenyl)-5-phenyloxazole (HPPO). The molecular structure of enol and tautomer forms are depicted in Scheme 1. We choose these systems to relate the dynamics to the nature of the change on the PES, covering three different types illustrated in Scheme 2. In Section 4, intermolecular proton transfer of α-naphthol in finite-sized clusters is discussed in relation to results from femtosecond and jet molecular beam studies. In the last section, relevance of these findings to condensed-phase reactions is briefly discussed.

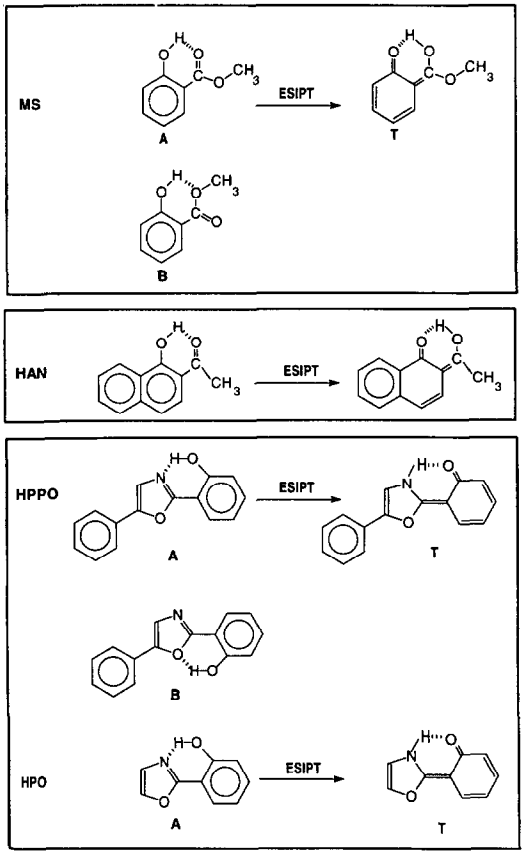

Scheme 1. Molecular structures of enol (A and B) and keto (T) forms of methyl salicylate (MS), 1-hydroxy-2-acetonaphthone (HAN), 2-(2′-hydroxyphenyl)-5-phenyloxazole (HPPO) and 2-(2′-hydroxyphenyl) oxazole (HPO).

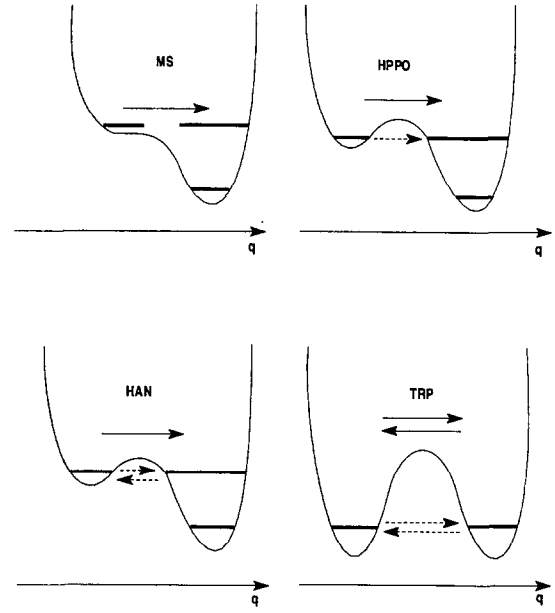

Scheme 2. Generic potentials of proton-transfer reactions of MS, HPPO, HAN, and tropolone (TRP).

2. Elementary dynamics

2.1. Proton and H-atom transfer reactions

Since the seminal work in solution by Weller [5], proton transfer is occasionally used synonymously with H-atom transfer. Depending on the molecular skeleton, the transfer can be described by a proton motion (the photoproduct has a zwitterionic character) or by a H-atom transfer (the photoproduct is the so called keto form). The characterization of the nature of the process is of great importance not only from the point of view of spectroscopy, but also

from the point of view of the reaction dynamics and relaxation pathways (time domain) of the tautomer.

In a proton-transfer process, a zwitterionic tautomer is formed, and such a process does not require rearrangment of the electronic charge distribution as compared with the process of H-atom transfer. For the latter, internal electronic and nuclear rearrangements take place for the stabilization of the keto tautomer. The former process might be described by a localized motion of the initial wave packet, from the neutral enol form to the ionic structure of the tautomer. In hydrogen-atom transfer, a more global delocalization is involved, utilizing other intramolecular coordinates.

Solvent effects (polarity and dielectric constant) on the fluorescence and structural considerations of the tautomer have been used to distinguish between both mechanisms [6,7]. Fluorescence spectra (excitation and dispersed emission) in jet-cooled molecular beams provided insight into the mechanism [8]. In solutions, direct evidence for the production of a keto form in 2-(2′-hydroxyphenyl)benzothiazole has been reported by Elsaesser and co-workers using time resolved IR spectroscopy [9].

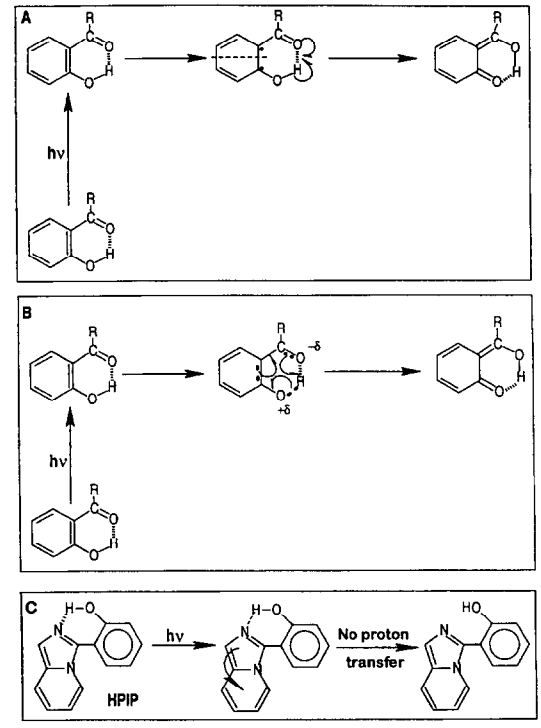

Scheme 3. Hydrogen-atom-transfer mechanism (panel A) with a biradicaloid species supposing to stabilize the keto form [10], and (panel B) with the involvement of a fast charge redistribution which simultaneously enhances the acidity and basicity of the OH and CO groups, respectively. Panel C: 3-(2′-hydroxyphenyl)imidazo[1,5-a]pyridine does not undergo proton transfer [7], an experimental observation contrary to what could be expected from the nodal plane theory. In A and B, R might be H, Me, NH_2, etc.

2.2. *Driving force of the internal motion*

The driving force of the photoinduced process comes from the drastic changes of the acidity and basicity of the involved groups or moieties of the system under study. When these changes (reflected in pK_a^*) are energetically favorable, the reaction can occur provided that no steric or strain reasons prevent the reaction. The ESIPT reaction originates from a π,π^* transition. By using nodal planes of wave functions of the HOMO and LUMO, Nagaoka and Nagashima proposed a 'different' description of the driving force origin of this reaction [10]. These authors suggest that, upon electronic excitation to the S_1 state, two delocalized π-electrons become localized on the two carbon atoms which bear the groups forming the IHB. The evolution toward the tautomeric form is predicted by symmetry considerations and orbital correlation arguments between the biradicaloid reactant and the final product (Scheme 3A). In the biradicaloid reactant, homolytic cleavage of the O–H bond and electronic rearrangement lead to a hydrogen-atom transfer. Both phenyl ring and IHB modes cooperate in the internal motion of the hydrogen atom.

However, this description does not explain, the experimental fact showing the great change of the acidity and basicity of the groups involved in the transfer. A simple nodal plane picture is not able to explain, for example, the lack of proton (or H-atom) transfer in 3-(2′-hydroxyphenyl)imidazo[1,5-a]pyridine (Scheme 3C) [7]. To better describe the occurrence or absence of proton-transfer reaction, we have to take into account the 'real' charge distribution within the whole system.

A simple mechanism can be drawn taking into account the electron withdrawing nature of the carbonyl and the mesomeric effect of the O–H groups, in agreement with the change of their proton affinity

in the excited state (Scheme 3B). Following this mechanism, the photon absorption rapidly brings an electronic cloud from the OH to the CO through the phenyl ring. This electron flow increases the acidity and basicity of hydroxyl and carbonyl groups, respectively, opening the way to a proton transfer reaction. Note that the electron flow in this mechanism implicates the phenyl ring and may involve a heterolytic cleavage of the O–H bond.

Recent findings, showing that the ESIPT reaction is not simply a localized process but instead includes other intramolecular modes, support this picture.

2.3. Potential energy surfaces

Semi-empirical quantum mechanical methods have been used to calculate one- and two-dimensional potentials for the ground and excited states of salicylic acid and derivatives with asymmetric OH...O bond [11]. These theoretical calculations concluded that the S_1 state potential of these compounds contains two inequivalent minima in contrast to the experimental result which suggests one minimum [12]. Very recently, more accurate results of calculations with the ab initio complete active-space self-consistent-field (CASSCF) method, and with second-order perturbation theory [13]; and with ab initio SCF and CIS levels with MP2 electron correlation have been reported [14]. The results are in agreement with the experimental observation, and bring more insight into the mechanism of ESIPT reactions. A PES with a single minimum corresponding to the formed tautomer is found [13,14]. The appearance of two minima in the earlier works is likely caused by use of approximate semi-empirical methods.

In o-hydroxybenzaldehyde (OHB) [13], it is found that the $^1\pi,\pi^*$ state is almost isoenergetic with the $^1n,\pi^*$ state. The PES of $^1\pi,\pi^*$ is found to be barrierless along the proton transfer coordinate. That of the $^1n,\pi^*$ state exhibits a significant barrier. The proximity of $^1\pi,\pi^*$ and $^1n,\pi^*$ may bring the system from the PES of the preparated state to that of $^1n,\pi^*$, which is not reactive. A fast PES crossing of this type can compete with the proton transfer rate. This coupling may also explain the slow proton transfer in OHB and HAN as compared to MS (see below). On the ground of experimental data, Acuña et al. anticipated the involvement of $^1n,\pi^*$ in the ESIPT dynamics of OHB [15–17].

Following a simplified one-coordinate description of the PES (Scheme 2), the ESIPT reaction can take place with (i) a barrierless transition from the enol form to the keto one (single-minimum distorted curve: MS), (ii) tunneling through a low-energy barrier (two minima and asymmetric PES: HPPO, and HAN), and (iii) 'deep' tunneling through a high energy barrier (two minima and symmetric PES: tropolone (TRP)). In the case of tunneling through a barrier, the process might be reversible. Barbara et al. have made a qualitative classification of the PES according to the symmetry of the molecule [18].

Molecular beam work, which was first reported in 1982 for MS [8], provided an approach for examining the *isolated* dynamics at the most elementary level. The earlier studies were made on the picosecond time scale in solutions and subsequently on the femtosecond time scale in beams and also in solutions. Since 1982 there have been numerous studies of MS and other new systems [6,7,19–22].

With the advent of the femtosecond methodology, it is possible to investigate real-time motion of the wave packet from the initially excited *enol well* to the *product tautomer well* [9,23–30], and to relate the dynamics to important features of the PES. From the theoretical and experimental (femtosecond and jet-cooled conditions) works on these systems and others, a multidimensional picture of the PES, taking into account the involvement of other intramolecular modes, emerges as a more realistic description of the reaction dynamics. The wave packet may find its way directly, or it may search through other modes toward the reaction coordinates, in analogy with direct and complex mode reactions [23,28–30].

2.4. Tunneling and multidimensionality

Quantum-mechanical tunneling can occur even in large systems with many degrees of freedom. The tunneling mechanism assumes a barrier in the PES [31]. Along one coordinate, the simplified picture of the potential can be drawn from a curve crossing involving an OH covalent bond and a Coulombic O^-H^+ ion-pair potential. H/D isotope effect on the proton (or H-atom) transfer reaction is usually used as a probe for the existence or non-existence of a

barrier on the PES, because tunneling probabilities are sensitive to mass change, which explains the strong proton/deuteron isotope effect.

In the oversimplified semiclassical model [31], the expression of the tunneling rate constant for bound-to-free (inverted) parabolic potential energy surface is given by

$$k_{H,D} = \nu_{H,D} \exp\left[-(\pi a_0/\hbar)(2mU_0)^{1/2}\right], \quad (1)$$

where $\nu_{H,D}$ is the OH (OD) vibrational frequency, m is the effective mass, a_0 and U_0 are the half width and the height of the barrier, respectively. This model is based on the occurrence of tunneling only when reactant and product states become degenerate.

The experimental evidences [12,19–21] for the multi-dimensionality of the PES lead to modification of this simplified model by introducing the coupling between the OH mode and the other degrees of freedom [32–36]. The two-dimensional tunneling model accounts for the following dependencies: deuterium isotope effect, vibrational excess energy, dependence on U_0 and a_0. In fact, U_0 and a_0 are strongly modified by the distance of the heavy heteroatoms involved in the transfer (we take as example O–N in phenol-ammonia), and these effects can be estimated by calculating an expectation value of the tunneling rate constant for each quantum state of the O–N stretch [33–36].

When the tunneling takes place at the zero level, k should be averaged over the zero-point vibrational motion of the O–N stretch;

$$k(\upsilon = 0) = \langle \phi_0 | k | \phi_0 \rangle , \quad (2)$$

where ϕ_0 is the harmonic wave function for the O–N stretch mode at $\upsilon = 0$. Then $k(\upsilon = 0)$ is given by

$$k(\upsilon = 0) = \nu(\alpha/p) \exp\left[q(q/p + 2a_0)\right], \quad (3)$$

$$\alpha = 4\pi^2 \mu \nu'/h,$$

$$q = -\pi^2 (2mU_0)^{1/2}/h,$$

$$p = \alpha - q/2a_0,$$

where ν is the OH vibrational frequency, μ and ν' are the reduced mass and frequency of the O–N oscillator, the other parameters were defined above. The probability of tunneling from the quantum states of the O–N stretch mode increases with the excess total vibrational energy. The rate constant should be averaged over energetically accessible quantum states of the O–N stretch mode. Bernstein and Kelley et al. [33] have developed expressions for vibrationally excited states of the heteroatoms stretch mode (O–N), and used them to account for the trends of experimental results.

If the system under study is solvated (cluster or liquid media), one has to take into account the variations due to the solvent (nature and size of the solvation shell) [33–37]. Syage [34] has discussed the approximations and limitations of the two-dimensional tunneling model and compared the experimental data of proton (deuteron)-transfer reaction of phenol and α-naphthol in clusters of NH_3 and ND_3. In addition to the tunneling barrier along the O–H coordinate, there is a barrier along the solvent coordinate. A minimum of four coordinates is needed. (1) The O–H coordinate, (2) the O–N coordinate, (3) the solvent coordinate taking into account the fluctuations in the relative energy of reactant and product caused by solvent modes; and (4) coordinates corresponding to product acceptor modes that reduce the energy gap between reactant and product.

Three variations of the tunneling model, relevant to systems discussed here, are described: (1) the bound–continuum model introduced originally by Bernstein and Kelley et al. [33], (2) the bound–bound activated solvent model developed by Syage [34], and (3) the same model, but extended by including product vibrations. The first model reproduces the relative rate constant as a function of vibrational energy (E_v), but does not take into account the variation of free energy (ΔG^0) of reaction for equilibration. The second model does not handle well the E_v and ΔG^0 dependence. When the vibrational coupling is introduced in the bound–bound model, a reasonable agreement with the dependence of rate constant on E_v and ΔG^0 is observed [34].

The multidimensionality of tunneling brings to focus an interesting concept for the propagation of the wave packet and the proton-transfer mechanism. In the initially excited configuration, a low tunneling barrier along the OH coordinate might exist. Because of the fast charge redistribution, which leads to the evolution of the wave packet along the other coordinates, the propagating wave packet might find an insurmountable barrier along these modes and get

trapped in the initial well or might couple with a non-reactive PES as that of n,π^*. This is a *non-reactive propagation mechanism* which might explain the absence of the ESIPT in 3-(2′-hydroxyphenyl)imidazo[1,5-a]pyridine where a strong IHB is formed in the ground state [7]. In elementary systems, such as methyl iodide, this type of motion was shown to account for a very large isotope H/D effect on the rate of C–I bond breakage [23].

The reverse reactive propagation mechanism is also possible depending on the structure and mode activity. The propagation of the wave packet along non-reactive coordinates might help to overcome the initial barrier in the OH coordinate, and in this case a reactive wave packet leads to the tautomer well. Interestingly, if IVR is not very fast, one might selectively control or induce these propagations by controlling the initial and final state, as prescribed by Manz's group for isomerization [37].

2.5. Radiationless transitions

The results of the semiempirical as well as of *ab initio* calculations associate the non-radiative process of the tautomer to the crossing between the potentials of ^{1}n,π^* and $^1\pi,\pi^*$ states. These calculations also suggested that the rate of crossing potentials of ^{1}n,π^* and $^1\pi,\pi^*$ states of the initial form competes with the rate of the proton transfer. On the other hand, the tautomer is initially produced with an excess energy (ca. 3000 cm^{-1}) and the new internal H-bond in the tautomer is weak and can be dissociated leading to a non-fluorescent state [19]. IVR, assisted by possible internal rotation and in solution solvent fluctuations, may enhance the coupling with dark and/or ground states.

3. Intramolecular proton-transfer reactions

3.1. Methyl salicylate (MS).

Salicylic acid and its derivatives are so far the most studied organic molecules showing ESIPT reaction [5,8,10–20,38–42], and MS is the most extensively studied one. Gas phase as well as liquid solution at room temperature and supersonic jet studies showed the coexistence, in both ground and excited states, of two conformers which we call here A and B (Schemes 1 and 4). The relative intensity of the two fluorescence bands depends on the excitation wavelength [38]. The structure of the excited state (B^*) is similar to that of the ground state, and the ultrafast change from A^* to the product tautomer T^* is responsible for the large Stokes shift (~ 6000 cm^{-1}) observed in the fluorescence spectrum.

Goodman and Brus [12] have shown that the spectroscopy of MS in Ne matrices at 4.2 K is not consistent with the simplified picture of the double-well potential. Picosecond and jet spectroscopies studied the system in an attempt to resolve the dynamics of the photo-intramolecular reaction [8]. Such studies were unable to give the rate constant for the hydrogen-atom motion, but gave some insight into the modulating modes in the transfer and the nature of the relaxation processes in the excited keto tautomer. A time constant of 10 ps has been suggested as the upper limit for the production of keto tautomer [12]. The supersonic jet data of Helmbrook et al. [39] have revealed the high-resolution spectra of both rotamers – A and B – and provided interesting information on the vibrational modes and isotopic (H/D) effects on the transfer. Nishiya et al. [40] have also studied MS and other related derivatives in durene at low temperature as well as in supersonic jets, and obtained information on the modes and potential of this reaction in the studied molecules.

The 0–0 transitions for the UV- and blue-fluorescing species (B^* and A^*, respectively) in the gas phase are at 309.6 and 332.8 nm respectively (Scheme 4). The enthalpy differences between A and B are 2.5 and 8.9 kcal/mol in ground and excited states [39], respectively. The ratio of the ground state populations of A to that of B was estimated as 70/1 [39]. Upon excitation to their respective 0–0 transitions, the observed fluorescence lifetime of B^* (non-hydrogen atom transfer) in gas phase is 1.1 ± 0.2 ns [16], and that of T^* (hydrogen-atom transferred form) in jet-cooled conditions is 12.0 ± 0.5 ns [8,39]. The UV fluorescence lifetime is independent of excitation energy contrary to the marked effect on that of the blue emission (see below). On the grounds of theoretical and experimental studies, the uv transition has been assigned to an nπ^* transition [39,41].

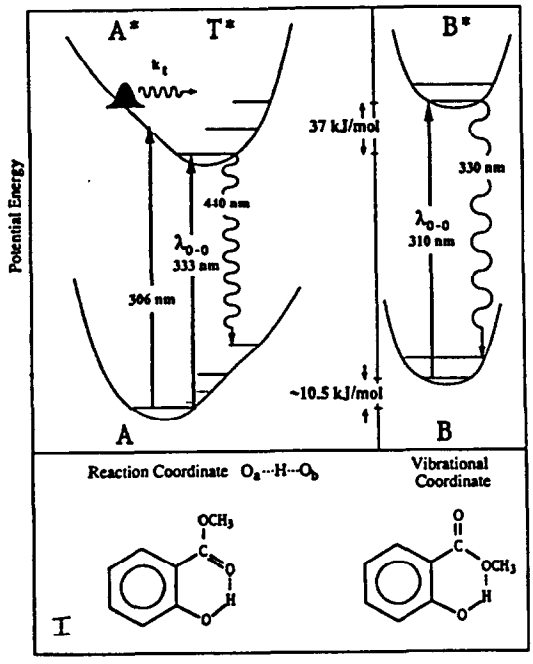

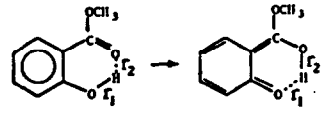

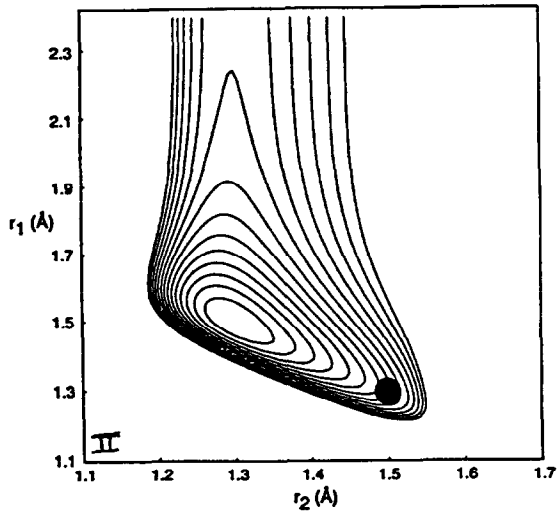

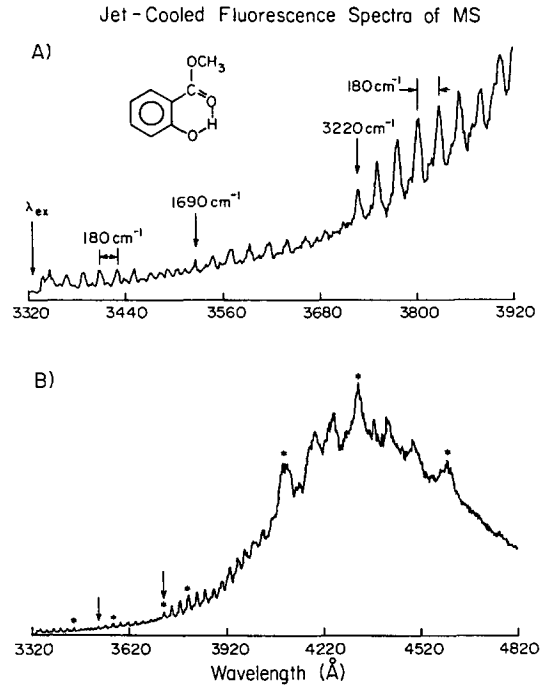

Fig. 1. Dispersed fluorescence spectrum of jet-cooled MS [8].

The blue one was attributed to a π,π^* transition [12,39].

The most important question to resolve is regarding the existence or non-existence of an energy barrier between the potentials of the initially excited enol form, A^*, and that of the formed keto tautomer, T^*. Theoretical studies indicated either a low barrier, or no barrier at all to the transfer. Felker et al. [8] reported a picosecond study of jet-cooled MS (Fig. 1) and explored the fluorescence decay rate of T^* as a function of excess vibrational energy of the initially excited A^*. No A^* fluorescence was observed indicating a fast and barrierless ESIPT reaction. One of the important findings obtained from the

Scheme 4. Panel I: schematic representation of the MS potential-energy surfaces for the 'blue' and 'UV' conformers (A and B) [19]. The vibrational coordinates involved are displayed [19]. The wave packet is approximately at the total available energy. Panel II: schematic of two-dimensional PES showing both the asymmetry in the potential and the exit barrier to the non-radiative channel. An energy-dependent propagating wave packet (see circle) can either be trapped in the well or exit as the system 'loses' the H-bond coordinate (see text).

high-resolution fluorescence spectrum of MS in supersonic jet is the observation of vibronic activity in the hydrogen-atom transferred form (Fig. 1).

Three types of modes have been observed in the red-shifted emission spectrum: (i) a low frequency mode, 180 cm^{-1}, built on the 0–0, C=O, and OH stretches, and suggested to be due to out-of-plane bending motion of the intramolecular 'ring' formed by the IHB; (ii) 1690 cm^{-1}, assigned to the ground-state carbonyl group stretch; and (iii) 3220 cm^{-1}, attributed to the hydroxyl group stretch. In the electronically excited state, A^*, these frequencies are decreased and become 176, 1094, and 2582 cm^{-1}, respectively, showing an increase in the C=O and O–H bond length. These changes are consistent with the production of ESIPT reaction in the enol form. On the basis of the correlation between the change in OH (and OD) stretch frequency and the change in bond length, a distance of hydrogen-atom transfer of 0.1–0.2 Å was estimated [39].

Theoretical calculations have shown that the shape of the excited-state PES along the OH coordinate strongly depends on the distance between the phenolic and carbonyl oxygen atoms [11]. Calculations in o-hydroxybenzaldehyde and o-hydroxyacetophenone, which are similar to MS as far as the reaction type is concerned, found that the reaction is better described as a H-atom transfer generating a keto tautomer than as a proton transfer which leads to a zwitterionic form [13,14]. Fluorescence lifetime measurements of MS in solution show a general correlation between the radiative rate constant of the tautomer and the dielectric constant of the medium, apparently consistent with a proton-transfer mechanism [38].

In the work by Felker et al., when excitation was beyond a threshold of ~ 1300 cm^{-1} of excess vibrational energy, the decay rate of the tautomer increased strongly, indicating the onset of an efficient radiationless transition of the excited keto form (Fig. 2). This observation is consistent with the behavior of the excitation spectrum at the same energy region, found in gas phase as well as in supersonic jet experiments, which shows a decrease in the fluorescence intensity and quantum yield, respectively [15].

This was our knowledge of the potential energy of the ESIPT reaction in MS and the relaxation of its tautomer. A femtosecond real-time probing of the dynamics of the ESIPT process, under collisionless

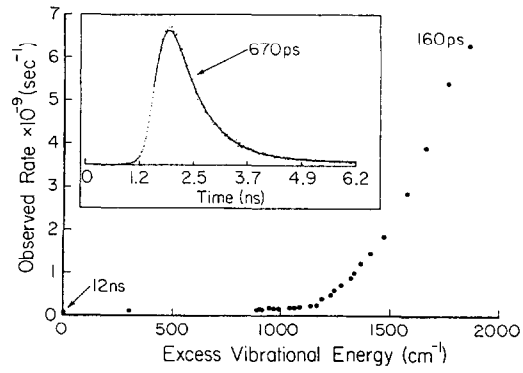

Fig. 2. Fluorescence decay rate constant of MS vs excess energy. The inset shows a typical decay and fitted curve corresponding to a point at the high energy end of the plot [8].

conditions, was needed in order to answer questions pertinent to the time scale of the H-atom transfer and the nature of vibrational phase space involved in the initial and final state of the transfer.

Herek et al. [19] reported such a study using femtosecond depletion spectroscopy. The excited state wave packet was created with a femtosecond uv pulse and the resulting dynamics was interrogated with a delayed red femtosecond pulse creating a depletion of the initially excited enol and product keto tautomer populations. The dynamics of H-atom (and D-atom) motion was followed, and the process was found to take place within 60 fs (Fig. 3). No isotope effect (OH/OD) has been observed, indicating a barrierless reaction in the A^* form (Fig. 3). The femtosecond experiment shows that the PES of the internal H-atom motion in MS in the excited state and along the OH coordinate is asymmetric and with a single minimum corresponding to the formed keto tautomer (Scheme 4).

The observations from the femtosecond to the picosecond time regime bring three issues into the dynamics of the reaction and the keto tautomer relaxation: (i) the nature of the initial coherent wave packet prepared at 3900 cm^{-1} excess energy, (ii) the evolution of the wave packet with time along the reaction coordinates (OH...O=C and others), and (iii) the relation between IVR and the spread of energy to the reaction coordinate and radiationless processes. In what follows we consider these issues and draw a detailed picture of the PES and dynamics.

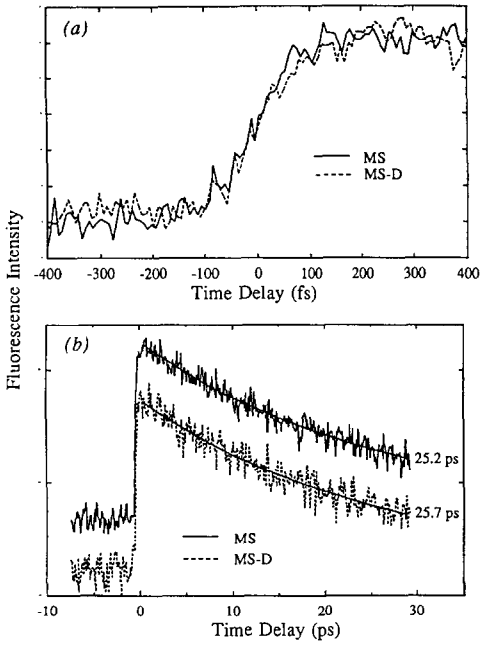

Fig. 3. Fluorescence depletion transients for (———) MS and (– – –) MS-D (deuterium effect) with short- and long-time scale [19].

At time zero, the wave packet is coherently prepared in the initial state and with time it reaches the reaction coordinate by femtosecond motion in (at least) two dimensions. Similar wave packet behavior has been observed in elementary and complex reactions [23,30]. In MS, the most probable second coordinate is the O...O bond. The reduction of this distance serves to produce the internal transfer during the compression phase of the OH vibration. The observed low-frequency 180 cm^{-1} progression in the dispersed fluorescence spectrum might be reduced to 176 cm^{-1} in the excited state giving a half period of 90 fs consistent with the observed time constant of the reaction. Note that the O–H bond stretch (2582 cm^{-1}) would give 13 fs for the motion.

Very recently, Vener and Scheiner [14] calculated the PES of the ground and lowest lying excited singlet states of o-hydroxyacetophenone at the ab initio SCF and CIS levels, respectively, with the incorporation of electron correlation into the computations via MP2. The calculated S_1 PES has a single minimum corresponding to the tautomer form where the proton has shifted from the hydroxyl group to the carbonyl one. The situation is inverted in the ground state. The enol form was found to be the most stable structure. Comparison of the fully optimized CIS geometry of both forms in S_1 reveals that the O...O distance suffers a shortening of 0.07 Å upon proton-transfer shift. This theoretical result is in good agreement with the observed fluorescence spectra [40]. The PESs of MS and its derivatives are better described by at least a two-dimensional picture where both O–H and O...O bonds are involved (Scheme 4).

The decay rate of the H-atom-transferred form was observed to be dependent on the total vibrational energy with a threshold of ~ 1300 cm^{-1} for a fast non-radiative process as it was found in earlier jet-cooled [8] and in solution phase works [12,15,38] (Fig. 3). No isotope effect was observed on the fluorescence decay rate of the tautomer (Fig. 3). Felker et al. [8] proposed that the onset may be due to the low frequency out-of-plane modes that are often active in 'floppy' systems like stilbene. However, the non-radiative decay rate has been found to depend only on the excess vibrational energy and not on the excitation of a specific mode [39]. The low-frequency 180 cm^{-1} mode observed in the dispersed fluorescence spectrum might be also active in the excited state in promoting non-radiative transitions through a coupling with isoenergetic vibronic n,π^* or ground states [19], or rovibronic couplings as in the channel-3 case of benzene [43]. Herek et al. [19] specifically related the behavior of the motion of the wave packet along the ESIPT reaction coordinate to the weakness of the formed IHB in the tautomer.

The produced excited tautomer is initially created in hot vibrational levels depending on the excess energy of excitation and on the energy difference between the relaxed vibronic states of the enol and tautomer forms in S_1. This gives a hot internal temperature to the unrelaxed tautomer which may induce the dissociation of the weak internal H-bond. The energy barrier for the non-radiative process (1300 cm^{-1}) is typical of H-bond energies [44] and is consistent with the required energy for the dissociation of phenol-benzene H-bonded complex (1400 cm^{-1}). Observation of hot tautomers in systems showing ESIPT reaction has been reported recently [45,46].

Scheme 4 displays the contour plots of the two-dimensional PES describing the asymmetry in the po-

tential and the rupture (or rotation) of the IHB as an exit channel to radiationless transitions in the tautomer. From the observed femtosecond dynamics to the picosecond relaxation of MS, the motion of the wave packet along the reaction coordinate at different vibrational energies and with a localized exit channel 'dissociation' is described. At low energies (below the 1300 cm^{-1} threshold), the packet spreads

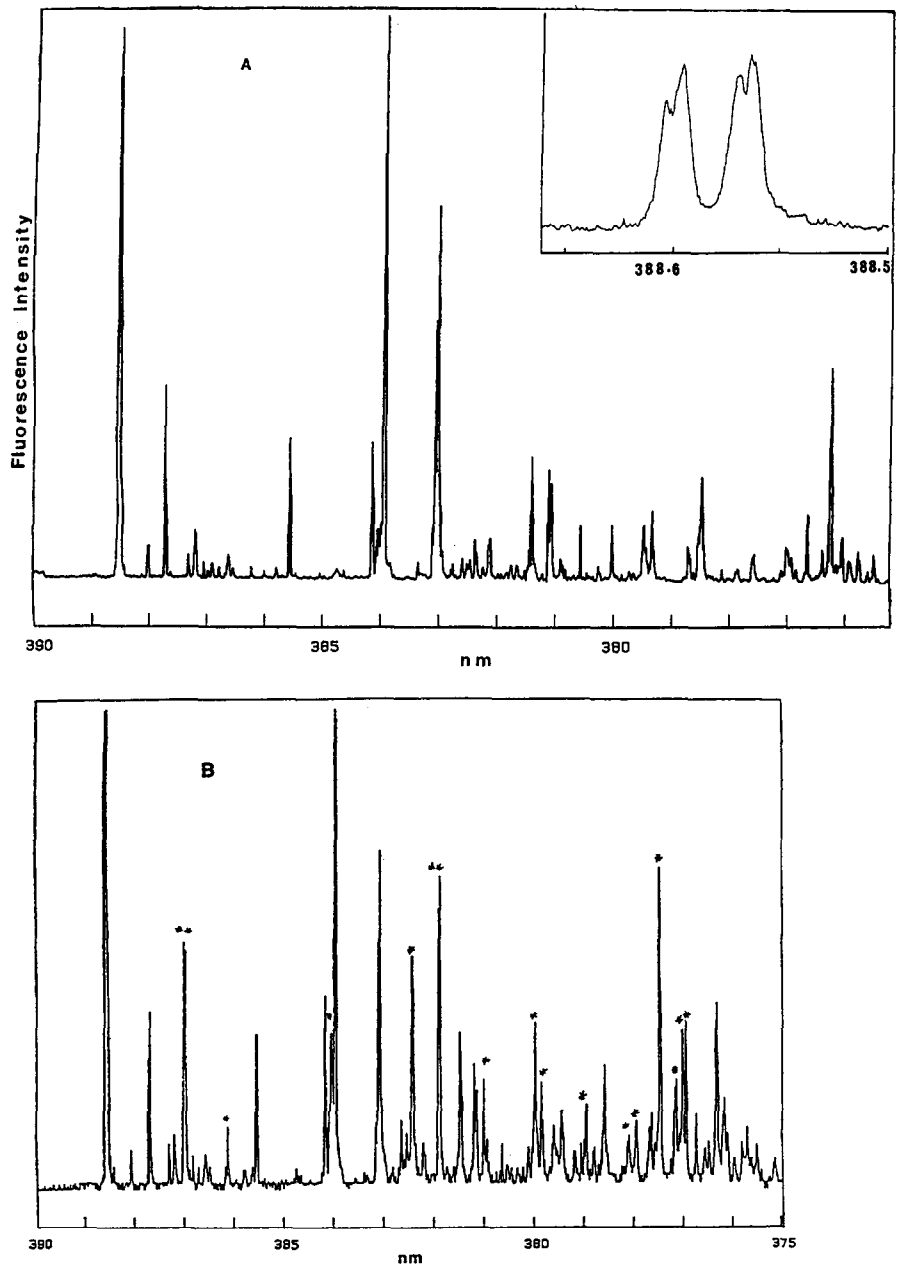

Fig. 4. Fluorescence excitation spectra of jet-cooled (panel A) HAN and (panel B) of a mixed sample of HAN and its OH deuterated analog DAN [20]. The inset in A shows the doublet structure and the rotational contour of the origin band of HAN, taken at a wavelength step of 0.0006 nm. The marked bands in B correspond to DAN.

along the reaction coordinate to the tautomer well and is trapped. At higher energies, the packet motion couples with dark states through a stretch/rotation internal H-bond dissociation mechanisms.

3.2. 1-Hydroxy-2-acetonaphthone (HAN)

As far as the OH and C=O groups being involved in an IHB, HAN is similar to MS (Scheme 1). However, the HAN skeleton does not contain a methoxy group, as in MS, and only one conformation is expected in gas phase or in non-hydrogen bonding solvents. This simplification might give other information on the ESIPT dynamics and the PES related to these kinds of molecules. With this in mind, Douhal et al. [20] carried out a supersonic-jet fluorescence study of HAN. The energy of the S_0–S_1 transition observed at 388.6 nm (Fig. 4) coincides fairly well with the onset of the absorption spectrum in cyclohexane (389 nm) and can be confidently assigned to the π,π^* transition of the planar conjugated system including the pseudo-aromatic chelate ring. The 0–0 band shows a doublet structure separated by 1.9 cm^{-1}. Hole Burning depletion spectra [47] have shown that the components of the doublet originate from different ground state species which may be assigned to rotational conformers of the CH_3 group. The fwhm of each component is about 1 cm^{-1} and the rotational envelopes exhibit well separated P and R branches with no prominent Q branch (Fig. 4A). At above 900 cm^{-1} from the origin, no fluorescence was detected indicating the onset of a very efficient non-radiative process in the jet. The spectrum displays narrow bands and is well resolved, and differs from that of the broad spectrum observed in the case of 2-hydroxyacetophenone [40–42], which has been explained in terms of a distorted PES in the excited state.

An H/D isotope exchange study, where the H-atom of the OH group was replaced by the D-atom isotope, allowed us to get more information about the nature of the PES and the modes affecting the transfer (Fig. 4B). While the low energy part of both HAN and DAN excitation spectra are identical (with a blue shift of 105 cm^{-1} in the DAN spectrum), the high energy part (above 320 cm^{-1} from the origin) becomes relatively congested. The difference in main band positions and intensity distribution may be the result of different vibronic coupling of the Frank–Condon excited state with a closely lying excited state.

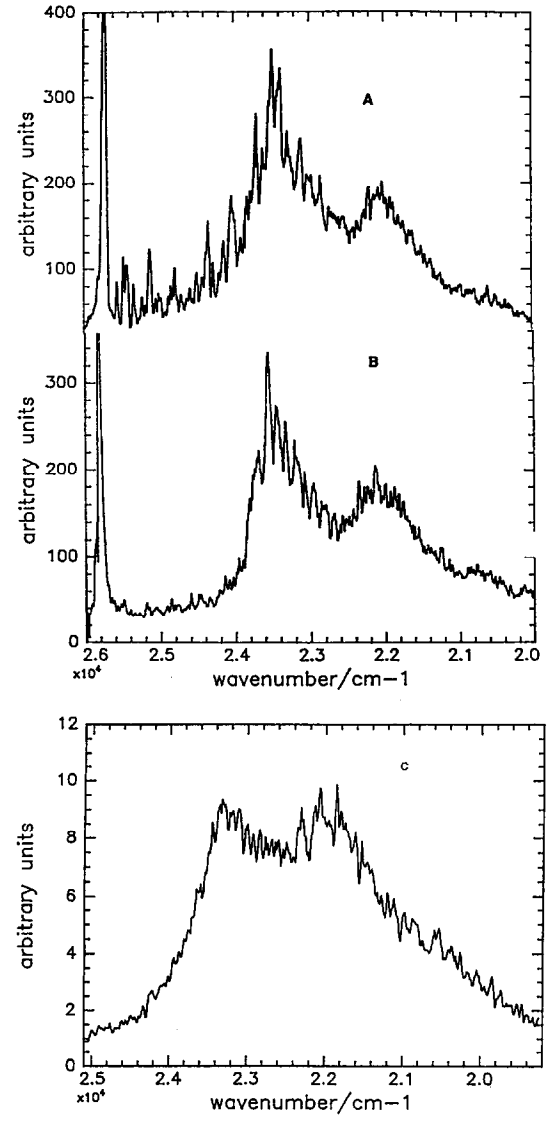

Fig. 5. Dispersed fluorescence spectra of jet cooled (A) HAN and (B) DAN at the origin of their S_0–S_1 transitions, and (C) of HAN excited at 26571 cm^{-1} (0^0 + 836 cm^{-1})[20].

The most striking observations have been found in the dispersed fluorescence spectra (Fig. 5). Excitation of HAN in the first excited 0^0 level gives a dual fluorescence emitted in two close but different spectral regions (Fig. 5A). The blue part of the spectrum

(~ 1400 cm^{-1} above the origin) displays a resolved vibrational pattern which bears in its first part mirror image symmetry with the excitation spectrum. The second part is composed by two broad bands red-shifted by about 2200 and 3500 cm^{-1} from the origin. Deuterium substitution of the hydrogen atom of the hydroxy group eliminates almost totally the blue and sharp fluorescence leaving the red and diffuse one unchanged (Fig. 5B).

The occurrence of ESIPT reaction in HAN (and DAN) is shown by the dual fluorescence and the isotope effect on the emission of HAN. The anomalous, observed isotope effect results in three findings: (i) confirmation of the existence of two different kinds of emission, (ii) the establishment of a tunneling mechanism by which the proton shifts from the enol well to the tautomer well, and (iii) an evidence for a double minimum PES in both ground- and excited-states. Indication of the evolution of the H-atom along the reaction coordinate is suggested by the vibrational frequencies in the ground and excited state of the enol form. For example, the 190 cm^{-1} vibronic frequency in the ground state is increased to 202 cm^{-1} in the excited state. This mode may be assigned to an out-of-plane bending vibration of the C–OH bond by analogy with hydroxyacetophenone. This behavior indicates a stronger force constant of this vibration in the excited state suggesting an increase in the strength of the IHB upon electronic excitation.

The bending of this part in the chelate ring may induce a variation of the O...O distance in the excited state and hence may be considered as an active mode (second coordinate in the PES) in the transfer. Assuming that the blue spectral shift of the 0–0 transition (105 cm^{-1}) of DAN relative to that of HAN is mainly due to the change in zero-point energies in S_1 and S_0 induced by deuteration, and using the observed ground state frequencies of OH (2750 cm^{-1}) and OD (2140 cm^{-1}) of both compounds in CCl_4, we estimated the O...O distance as 2.6 Å, a value indicating a strong IHB in the ground state.

The abnormal isotope effect is interpreted by invoking structural and electronic considerations. Two kinds of observations have been made when comparing the excitation spectra of HAN and DAN: (i) the appearance of new bands upon deuteration,

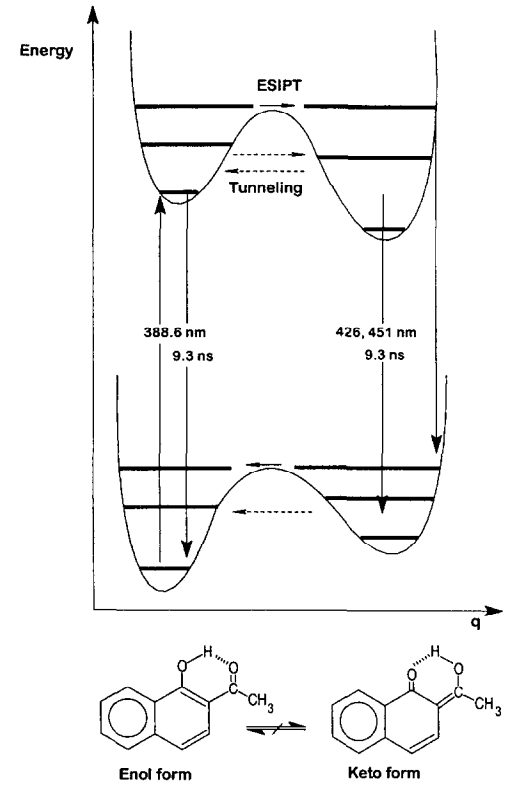

Scheme 5. Double-well potentials of the H-atom transfer in HAN in both ground and excited states. The given data are from a jet cooled molecular beam experiment (see text).

and (ii) the change in the remaining bands relative intensity indicating a modification of the coupling mechanism between vibrational modes which open the way to the formation of the tautomer. Hence, besides the OH mode, other intramolecular degrees of freedom are involved in the transfer, and the most active one is the O...O stretching vibration. The increased density of states in DAN enhances the rate of the transfer and shifts the equilibrium between both excited forms to the tautomer one.

The dispersed emission spectrum of HAN also shows that each ground state minimum is characterized by its own vibrational structure, and that they correspond to different species. Hence, the PES of ESIPT reaction (and back-proton transfer reaction in the ground state) in HAN (and DAN) contain two minima with an energy barrier contrary to those of MS (Scheme 5). The existence of an energy barrier in the PES in the excited state was also confirmed by

the absence of the enol fluorescence of HAN when an excess excitation energy above ~ 300 cm^{-1} was used (Fig. 5C). This amount is the energy barrier in the PES of HAN. The absence of the enol fluorescence in DAN – unusual isotope effect – indicates that H/D isotope substitution changes the electronic structure of the excited enol form in accordance with the difference in distribution and intensity of the high energy part of the excitation spectra. The band maxima of the proton-transferred form (426 and 452 nm) are not affected by the isotopic substitution, and the 426 nm part is overlapped by a progression involving intervals of 120 cm^{-1}, while the second one is diffuse. The envelope of the FC distribution of this mode indicates that the excited state tautomer geometry is displaced relative to that of the ground state along a coordinate involving a low-frequency motion which is not strongly affected by deuteration.

The mechanism of the H-atom motion in the electronically excited HAN can be described by an asymmetric PES with a barrier energy of ~ 300 cm^{-1}. The observed abnormal isotope effect on its fluorescence is believed due to structural and electronic changes induced by the deuterium atom.

The fluorescence lifetime of HAN 0^0 level (9.4 ns) does not depend on the observation wavelength, set either in the enol part (400 nm) or in the tautomer bands at 426 and 451 nm, suggesting an equilibrium between both forms. When exciting the 836 cm^{-1} vibronic band, the lifetimes become shorter than 6 ns, indicating the onset of an efficient non-radiative channel at this threshold of energy, and consistent with the falloff of the fluorescence intensity in the excitation spectrum. The lifetime of the DAN tautomer is longer (13 ns) than that of HAN (9.4 ns), indicating a different IVR process which leads to dark states.

It is interesting to compare the PES and dynamics of ESIPT in MS and HAN. In MS, ESIPT dynamics has been observed to occur within 60 fs. That of HAN has not yet been directly measured [work in progress], but a time constant in the picosecond time scale is mostly expected as the enol fluorescence (ns decay) was observed.

The difference between HAN and MS H-atom transfer dynamics might be due to the fact that a larger intramolecular electronic redistribution is necessary in HAN for the changes in pK_a's of the –OH and of the C=O groups leading to the occurrence of an ESIPT reaction. It is worth noting that the greater the redistribution, the higher is the acidity of the OH group ($pK_a^* = 4.1$ and 0.5 for phenol and α-naphthol, respectively). On the other hand, by comparing the Stokes shift of both MS and HAN (~ 6000 versus ~ 3000 cm^{-1}), the difference of the spectroscopy of these molecules rests on the energetics of the reaction. In the case of MS the reaction is much more exothermic (and the PES more distorted) than in the case of HAN. The energy gap between the enol and keto forms of MS is most probably greater than that in HAN. This difference should be reflected in the dynamics of the reaction.

3.3. 2-(2'-hydroxyphenyl)-5-phenyloxazole (HPPO)

2-(2'-hydroxyphenyl)benzoxazole (HBO) is also one of the most studied molecules showing ESIPT reaction [25,48–51]. Recently, Ernsting and coworkers [25] reported a femtosecond study of the proton-transfer dynamics in solution and the fluorescence excitation spectrum under jet-cooled conditions. The reaction (in solution) has been found to occur within 60 fs [25]. The excitation spectrum observed under jet cooled conditions does not allow for direct information or more details on the mechanism and PES of the reaction. 2-(2'-hydroxyphenyl)-5-phenyloxazole (HPPO) (Scheme 1), a molecule which belongs to the oxazole family, exhibits ESIPT reaction, and a spectacular effect of the H/D exchanged isotope on the fluorescence excitation spectra in a jet-cooled molecular beam [21] (Fig. 6).

First, we note that HPPO in solution coexists under two stable rotamers (Scheme 1), like HBO [48] and MS. Under jet-cooled conditions, no fluorescence from OH...O form has been detected, and only the OH...N bridged rotamer (called from here HPPO) which can give ESIPT reaction was observed [21].

The fluorescence excitation spectrum of HPPO consists of strong, diffuse and broad bands [21] starting from an origin centered at 29852 cm^{-1} (Fig. 6a). That of 2-(2'-methoxyphenyl)-5-phenyloxazole (OMePPO), where the H-atom in the OH group is substituted by a methyl group, shows a high vibrational structure and starts at 30376 cm^{-1}. The electronic delocalization introduced by the IHB in HPPO relative to OMePPO is reflected by the energy differ-

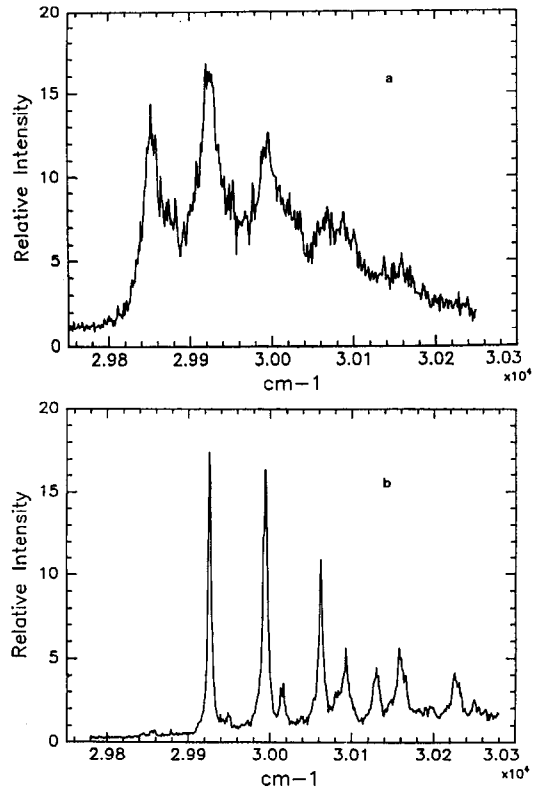

Fig. 6. Fluorescence excitation spectra of (a) HPPO and (b) DPPO in a jet cooled molecular beam [21].

ence (524 cm^{-1} or 1.5 kcal/mol) between both 0–0 electronic transitions in these molecules [21]. In HPPO, solvation by cyclohexane induces a relative stabilization of the excited-state by 830 cm^{-1}.

The excitation spectrum of the DPPO is a much narrower spectrum, but with the same vibrational pattern as that of HPPO. The dispersed fluorescence spectrum – exciting 0–0 band or others – shows a highly Stokes shifted band starting at ~ 6500 cm^{-1} from the 0–0 transition (Fig. 7). The red-shifted and broad fluorescence band is a signature of the occurrence of ESIPT reaction in the initially excited enol form. The final state most likely has a keto character, as evidenced in the case of 2-(2′-hydroxyphenyl)benzothiazole using picosecond time resolved IR spectroscopy [9].

As mentioned above, HPPO and DPPO do not show any resonant fluorescence (Fig. 7), contrary to OMePPO – a molecule which cannot give ESIPT reaction – which exhibits a very strong structured 'normal' emission starting from the 0–0 transition [21]. Hence, the H-atom motion in HPPO occurs on a time scale much shorter than that of the radiative decay time of the OH...N closed enol form. The 0–0 transition of DPPO is 75 cm^{-1} blue shifted from that of HPPO, and suggests a strengthening of the OH...N IHB upon electronic excitation. Assuming that this spectral shift is mainly due to an effect of the isotope on the zero-point energies in both ground and excited states, the frequencies of OH and OD stretches are reduced from 3050 and 2250 to 2455 and 1805 cm^{-1}, respectively. The onset of a very efficient radiationless transition at ~ 400 cm^{-1} above the origin did not allow to observe the activities of the OH and OD modes in the transfer. However, interesting information could be reached from the isotope effect and the progression shown in the excitation spectra.

We now consider the mechanism of ESIPT reaction in a jet-cooled beam of HPPO, using the isotope effect, the progressions in the excitation spectrum (67 and 164 cm^{-1}), and the observed fluorescence upon exciting the OH...N enol form. One of the most important findings reached by the isotope effect (OH/OD) is the drastic narrowing of the bands of the excitation spectrum upon deuteration (Fig. 6b). Since the vibronic bands exhibit typical Lorentzian shapes, one may infer that the broadening of the bands of both HPPO and DPPO is homogeneous in nature (Fig. 8). Under identical experimental condi-

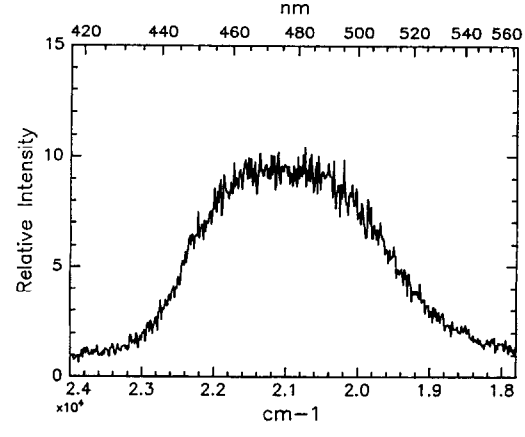

Fig. 7. Dispersed fluorescence spectrum of HPPO excited at the 0–0 band [21]. A similar spectrum was obtained for DPPO [21].

tions, the rotational contour of the 0–0 transition of OMePPO is much more narrow than that of DPPO (Fig. 8), and a convolution taking into account the laser profile and the rotational contour of the transition was not necessary. From the equation

$$\mathrm{fwhm}_{\mathrm{hom}} = (2\pi c\tau)^{-1}, \qquad (4)$$

where $\mathrm{fwhm}_{\mathrm{hom}}$, c, and τ are the full-width at half the maximum intensity of the vibronic band, the speed of light, and the lifetime of a given vibronic state of the isolated molecule, respectively, the time constants of the ESIPT reaction were calculated. The estimation gives an upper limit of the rate constant, $k_{\mathrm{ESIPT}} = \tau^{-1}$, in these vibronic levels of HPPO and

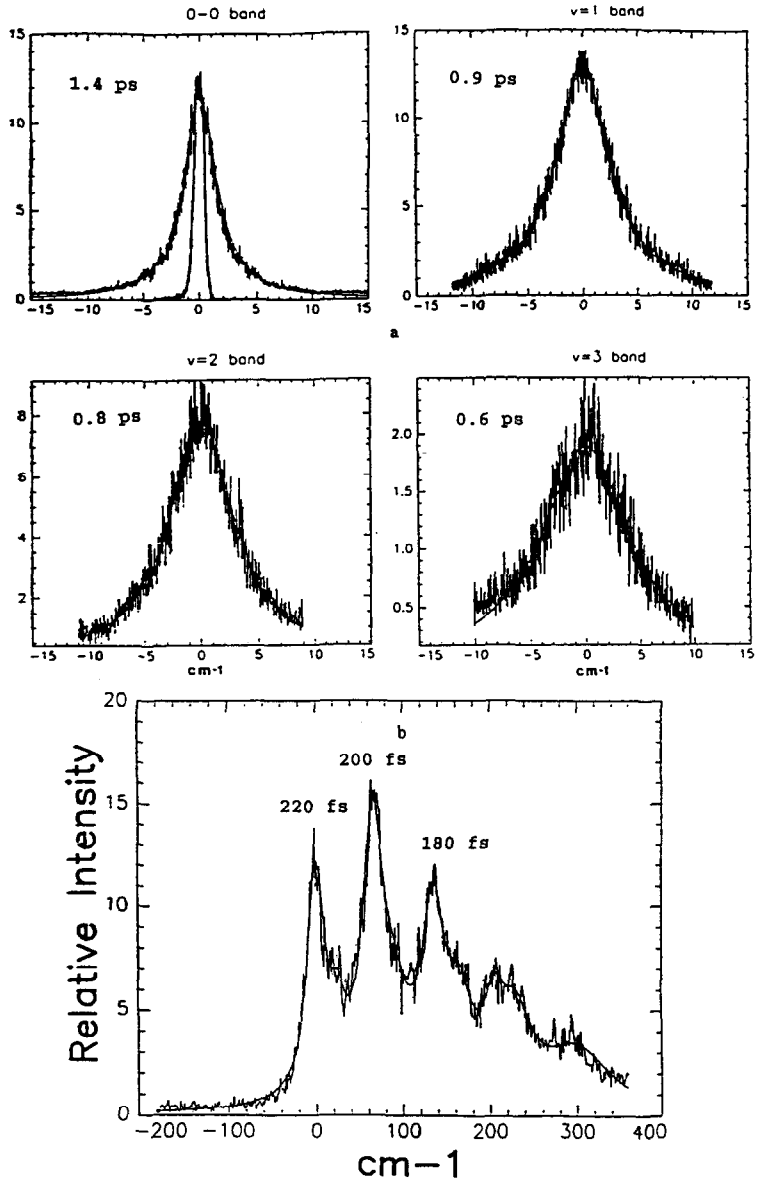

Fig. 8. (a) Experimental and Lorentzian-fitted contours of the main vibronic bands of DPPO. Also is shown in the first panel the experimental 0–0 band of OMePPO superimposed on that of DPPO. (b) Experimental and fitted Lorentzian fluorescence excitation spectrum of HPPO [21]. τ is the lifetime of the vibronic band (see text).

DPPO (Fig. 8). Several conclusions can be reached from the isotope effect and the estimation of k_{ESIPT}.

(i) The ESIPT reaction in HPPO irreversibly occurs in the femtosecond time scale; the time constant for the 0^0 level is ~ 220 fs. This ultrashort time related to the ESIPT process explains the lack of the fluorescence from the initially excited enol form.

(ii) Deuteration of HPPO (OH/OD) leads to a significant decrease of k_{ESIPT} by a factor ranging from 4 to 6, depending on the excess energy. The isotope dependence is a signature of the tunneling mechanism and hence the existence of two minima in the PES of HPPO. The absence of any resonant fluorescence from the enol form combined with the isotope effect suggest that the internal motion can be better described by a large asymmetric PES along a reaction coordinate with a low energy barrier. The rapidity of the reaction even at the lowest vibronic level (~ 220 fs), and the onset of an efficient radiationless transition at ~ 400 cm^{-1} above the 0–0 transition did not allow for measurement of the height of the barrier, however. On the basis of the simplified mono-dimensional model of tunneling which uses equation 1 and the excess energy dependence of k_{ESIPT}, an energy barrier higher for HPPO (2950 cm^{-1}) than for DPPO (2180 cm^{-1}) has been calculated. However, the difference between these barrier heights does not reproduce the expected one from the zero-point energy of OH and OD oscillators ($U_{HPPO} = U_{DPPO} - 320$ cm^{-1}).

(iii) The rate constant increases slowly in HPPO but more rapidly in DPPO, indicating a larger density of states in the deuterated molecule than the hydrogenated one, and this is the result of the large decrease of the frequencies localized on the OD bond relatively to those on the OH one.

One of the comprehensive approaches to understanding the proton-transfer dynamics is that using the Fermi golden rule (FGR) applied to these kinds of reactions [21,52]. In this approach the reaction is described as a non-radiative transition with the excited enol and keto forms as the initial and final states in an isoenergetic transition. The rate constant is thus given by

$$k_{FGR} = (4\pi^2/h) C_{if}^2 \rho , \tag{5}$$

where C_{if} is the matrix element of the interaction between the initial i⟩ and final f⟩ states coupled in the transfer, and ρ is the density of final states isoenergetic to the initial states. The coupling term C_{if} is obtained from the theory for an O–H symmetric double-well potential with an inverted parabolic barrier as [31,32]

$$C_{if} = (h\nu_{H,D}/2\pi) \exp\left[-\pi^2 (a_0/h)(2mU_0)^{1/2} \right] . \tag{6}$$

Because of the many low-frequency modes due to the skeletal torsion and bending modes as well as H-bond deformation, the density of states in the excited keto form might be very large at high vibronic levels and not affected by the addition of successive 68 cm^{-1} quanta. As indicated above, H/D exchange might affect the density of states in the keto form resulting in different excess energy-dependence of the ESIPT reaction rate constant in agreement with the experimental observation.

The progressions of 67 and 164 cm^{-1} are not affected by the H/D isotope exchange, however. This suggests that the corresponding low frequency modes are not sensitive to the OH deuteration and may not involve localized motions on the OH...N hydrogen bond. This explanation is supported by the presence of similar low-frequency bands in the excitation spectra of 2,5-diphenyloxazole, and 2,5-diphenylfuran [53]. In HPPO, as in DPPO, the progression of 67 cm^{-1} has been suggested as resulting from the $\Delta\nu = 2$ transition of a phenyl out-of-plane torsion motion involving a ~ 33 cm^{-1} fundamental frequency. The 164 cm^{-1} frequency was assigned to an out-of-plane deformation or to an in-plane bending vibration modifying the angle between the oxazole and the hydroxyphenyl parts.

The shortening of the vibronic lifetime or the increase of the rate constant observed when different members of the 68 cm^{-1} progression are excited may be due to a decrease of the tunneling parameters (height and width of the barrier) induced by this low-frequency oscillation in the excited state of the enol form. This oscillation is not expected to be directly involved in the proton-transfer process, as it is not affected by the OH deuteration. The oscillation period corresponding to this progression mode is ~ 500 fs, which is between the experimental times for H-atom and D-atom transfer obtained from spectral broadenings.

Several studies have explored the possible influence of the phenyl motion in the ESIPT reaction of 3-hydroxyflavone and derivatives [54]. A recent femtosecond study carried out by Harris and co-workers [27] did not observe any evidence of the coupling between the phenyl motion and the proton-transfer rate. In fact, the internal flight of the proton is too fast for the electronic change induced by the phenyl motion to be important in the dynamics. However, one should consider that the phenyl substituent can change the density of states in both forms and hence affects the rate of the proton-transfer as suggested to occur in HPPO and DPPO. In fact, Itoh's group found an influence of the torsional motion as well as electronic effect of the phenyl (and naphthyl) substituent at the 2-position of the γ-pyrone ring, in the bandwidth of the 0–0 transition of 2-substituted 3-hydroxychromones in jet-cooled molecular beams [54]. In HPPO, it would be interesting to examine the phenyl group effect on the proton-transfer dynamics by comparing its real-time probing reaction with that of 2-(2′-hydroxyphenyl)oxazole (HPO) (Scheme 1), where the phenyl substituent is not present in the molecular frame.

To get a better description of the PES of HPPO, we have to take into account other intramolecular vibrational modes which can modulate the transfer from the enol potential to the keto one. Very recently, Moreno et al. [55] carried out theoretical calculations on the closed-enol, transient, and tautomer forms of 2-(2′-hydroxyphenyl)oxazole (HPO) (Scheme 1) in both ground and excited states, and at the ab initio SCF and CIS levels. The results show that in the course of nuclear motions in the excited state from the enol well through the transition state (TS^*) and to the tautomer (T^*) well, the most affected distance, apart those of O–H and N–H bonds, is the N...O one. From S_1 to TS^* states, it is reduced by 0.31 Å, and later from TS^* to T^* states it is increased by 0.27 Å. As the N...O distance is the most affected mode, it is reasonable to take this bond as the second coordinate in the two-dimensional picture of the PES of the ESIPT reaction in HPO.

As HPPO and HPO are very similar as far as the involved moieties in the proton transfer are concerned, the theoretical result on HPO is in good agreement with the experimental observation made for HPPO in jets: existence of a barrier and involvement of the N...O mode in the transfer. In fact, in that work, Douhal et al. [21] reported a scheme of the PES with the O–H and O...N coordinates taking into account the existence of a small energy barrier and the compression of the O...N distance; and the theoretical work strongly supports this picture. The PES of ESIPT reaction of HPPO is shown in Scheme 6 to highlight these points.

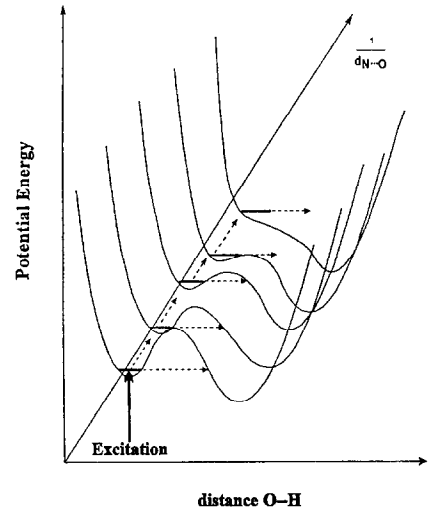

Scheme 6. Schematic representation of the PES for the phototautomerization of HPPO [21]. The system evolves along the O...N coordinate reducing the width and energy of the barrier, and modulating the other intramolecular vibrational modes leading to a tunneling and/or classical movement of the system along the OH coordinate from the enol to the keto wells (see text and Scheme 1 for the molecular structures).

3.4. Intermolecular proton-transfer reactions

The system of interest here is a reaction between the excited solute AH^* and the finite-sized solvent S_n ($n = 1,2,...$ is the number of molecules)

$$AH^* \cdot S_n \rightleftarrows [A^{*-}...S_nH^+] \rightarrow A^{*-} + S_nH^+ , \quad (7)$$

where AH stands for α-naphthol (α-NpOH) and S_n for ammonia, piperidine or water molecules. The reversibility of the first process has been considered in bulk studies [56,57] and in finite-sized cluster dynamics [35,58].

Time-resolved fluorescence and mass-selected spectroscopies have been used to study the dynamics of the reaction [35,58]. Fig. 9 shows a typical time-

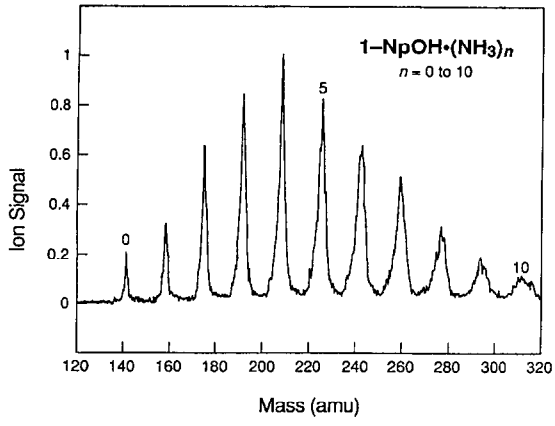

Fig. 9. Multiphoton ionization time-of-flight mass spectrum of α-naphthol$\cdot(NH_3)_n$ [58].

of-flight mass spectrum for α-NpOH $\cdot (NH_3)_n$ clusters obtained with a laser wavelength of 322 nm. The picosecond time-resolved transients for the clusters α-NpOH $\cdot (NH_3)_n$, α-NpOH $\cdot$ (piperidine)$_n$, and α-NpOH $\cdot (H_2O)_n$ are shown in Fig. 10.

The bare-molecule lifetime has been found to be 60 ± 2 ns. For $n = 1$ ammonia cluster, the lifetime is reduced to 38 ± 1 ns. For $n = 2$, two clusters were identified; the spectrally bluer isomer has a lifetime of 43 ± 2 ns, while the spectrally redder isomer has a lifetime of 39 ± 1 ns. When the clusters contain three molecules of ammonia and are interrogated at the lowest energy studied, a two-component decay appears. The fast decay component has a lifetime of 52 ps, and the slow one has a lifetime of 1.2 ns.

A similar trend has been observed for the piperidine clusters (Fig. 10b). No proton transfer occurs when $n = 1$, while for $n = 2$ or 3, picosecond dynamics with a decay of 65 ps was measured. It is noteworthy that, for $n = 3$ clusters, the transient decay reaches the zero background within less than 500 ps. Clusters of water up to $n = 21$ do not show any dynamics which could be assigned to the proton-transfer process (Fig. 10c). The occurrence of proton transfer by a tunneling mechanism has been observed by measuring the decay of clusters of α-NpOD $\cdot (ND_3)_3$ (Fig. 11).

These results show a clear dependency of the proton transfer dynamics of α-NpOH on (i) the nature of the solvent, (ii) the mass of the transferred particle (H/D), and (iii) most importantly on the number (size) of the solvent molecules. The critical numbers of the solvent molecules to be used are 3 and 2 for ammonia and piperidine, respectively [35,58]. No proton transfer has been observed for water up to 21 molecules.

The energetics and dynamics of the reaction are determined by the local structure of clusters formed in a molecular beam. For α-NpOH $\cdot (NH_3)_3$ clusters, several geometrical isomers or conformers are possible. In fact, some ammonia molecules may solvate the ring and affect the energetics involved in the proton-transfer dynamics, thus making an interplay between the structure and the dynamics. Felker's group has shown that, in two-ammonia clusters, both NH_3 molecules are H-bound to the OH group in one isomer, while for the other isomer the results suggest an NH_3 bound to the α-NpOH ring [59]. For 3 molecules of ammonia several isomers could exist in the beam, and in one of them NH_3 trimer is bound to the OH group of α-NpOH [59].

From the point of view of energetics, the enthalpy of the reaction [58] is

$$\Delta H_{PT}(n) = \left[\Delta H_{dep} + \Delta H_{sta}(n)\right] - (PA_n + V_n), \tag{8}$$

where ΔH_{dep}, $\Delta H_{sta}(n)$, PA_n, and V_n stand for the enthalpy of deprotonation (~ 327 kcal/mol [60]), the enthalpy due a stabilization energy for the neutral α-NpOH through H-bonding with ammonia (~ 14 kcal/mol for $n = 3$ [61]), the proton affinity of $(NH_3)_n$ (~ 238 kcal/mol for $n = 3$ [60]), and the electrostatic stabilization energy of the ion-pair product of α-NpOH $\cdot (NH_3)_n$, respectively. For 3 molecules of ammonia, the electrostatic contribution in the energetics should be at least ≈ 103 kcal/mol [58] for the formation of the H-bond complex and thus the occurrence of the proton-transfer process.

From the point of view of dynamics, one should consider the rate constants of the processes described by Eq. (7). Kim et al. [35,58] obtained the experimental decay for 3 molecules of ammonia, with femtosecond resolution, and also examined the excess vibrational energy and the isotope (OH/OD) effect on these rates (Fig. 11). For an excess energy of 200 cm^{-1}, the time constants, τ_1, τ_{-1}, and τ_2 related to these processes for the transfer of H-atom (D-atom) are 71 (275), 200 (370) and 910 (> 1120)

ps, respectively. For an excess energy of 1540 cm^{-1}, these times become 35 (143), 106 (357) and 164 (1200) ps, respectively.

The results show that the fastest rate constant of the transfer k_1 $(1/\tau_1)$ decreases with D-atom substitution and increases with the total energy. The rate

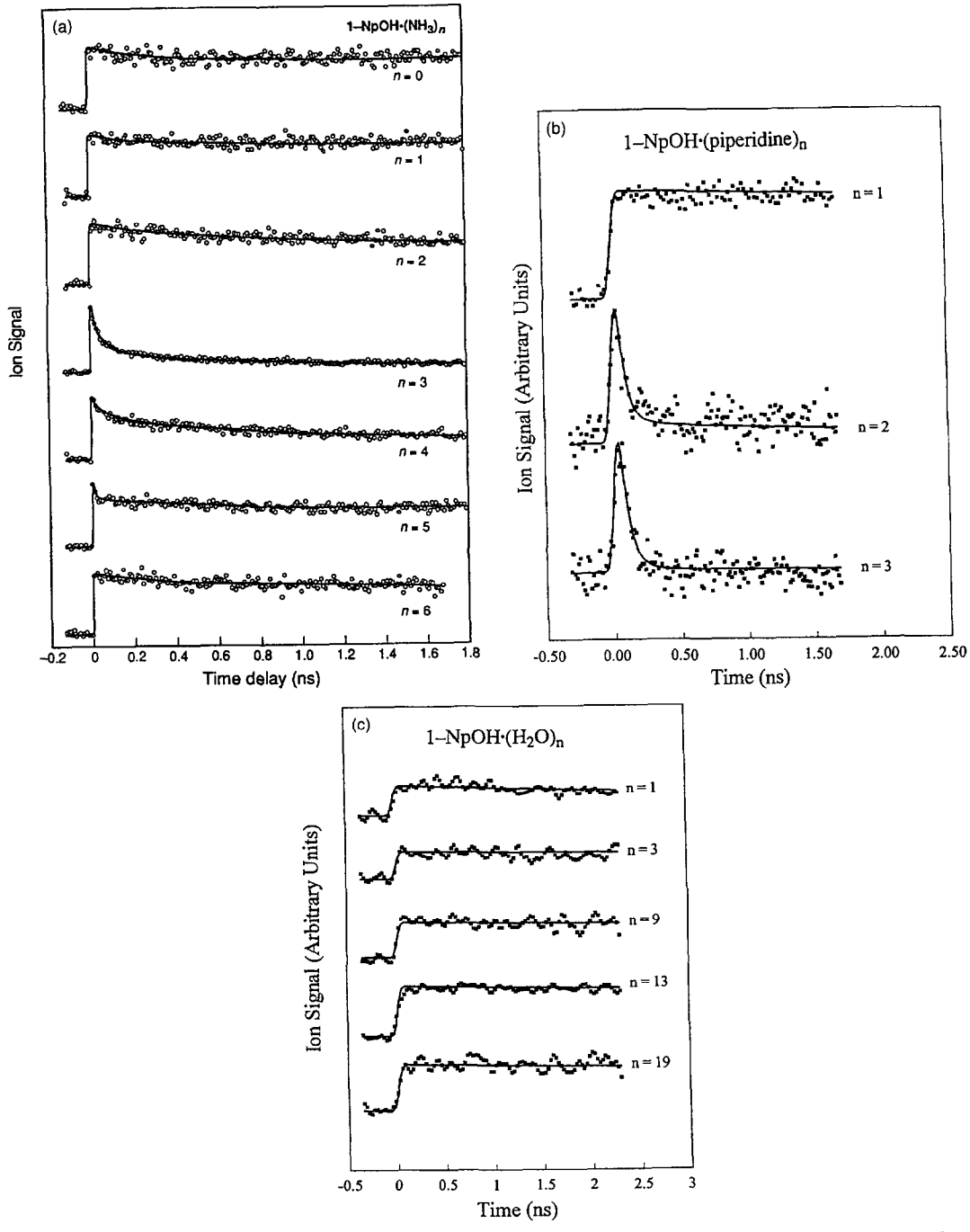

Fig. 10. Pump–probe transients for clusters of α-naphthol (NpOH) with (a) ammonia (NH_3), (b) piperidine and (c) water [35,58].

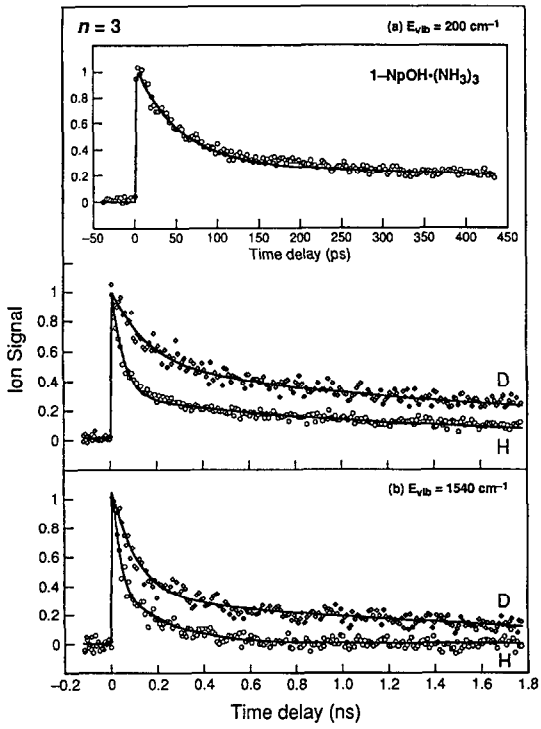

Fig. 11. Subpicosecond excitation and transient decays for α-NpOH·$(NH_3)_3$ and α-NpOD·$(ND_3)_3$: (a) Pump/probe wavelengths are 320/340 nm and (b) 307/340 nm. Excess vibrational energies are relative to the origin at 31050 cm^{-1} for the $n = 3$ cluster [35,58].

constant of the reverse process, k_{-1} $(1/\tau_{-1})$, is smaller than k_1, and within the time scale of both processes, IVR may play a role on the dynamics. The rate of the irreversible process, k_2 $(1/\tau_2)$, is the smallest one. Some of the measurements have been made near the origin where the IVR process is expected to be on a longer time scale, and hence could be excluded in the analysis. The IVR rate is expected to increase with (i) the excess energy as the density of states increases in α-NpOH, (ii) the number of degrees of freedom due to clusters modes by increasing the number of solvents molecules, and (iii) H/D substitution which decreases the vibrational frequencies. The results show the dependence on excess vibrational energy, consistent with this expectation, and tunneling which involves more than one coordinate.

Ando and Hynes showed, by using molecular dynamics, that tunneling is not significant in the first step of the proton transfer reaction between HCl and water [62]. The description of the isotope effect is based on a one-dimensional potential, and it does not take into account the explicit solvent coordinate involved in the reorganization. As discussed by Kim et al., one should take into account in the dynamics of this process the interplay between the influences of the cluster size, the solvent reorganization and the tunneling mechanism [35,58].

Another system of interest in size specific time-domain studies which has shown excited-state proton-transfer reaction is phenol · $(solvent)_n$ clusters [30,34,36]. Syage's group has investigated several issues of the process in a variety of solvents. Valuable spectroscopic and dynamic information on the stepwise solvation properties of the proton transfer in this system was obtained. Similarly to the α-NpOH · $(NH_3)_n$ clusters, a critical solvent size for the process (5 molecules of ammonia) has been found [34,36], and Syage has provided details of the nature of the tunneling process in these systems.

4. Relevance to the condensed phase

In ESIPT reactions, the internal motion of the proton (or H-atom) occurs on the femtosecond time scale, faster than that of the solvent reorganization. The displacement within the IHB does not need a relay with the solvent molecules contrary to what occurs in some kinds of intermolecular proton transfer reactions as those of 7-azaindole [63] and 7-hydroxyquinoline [64]. Within this context, the rate of ESIPT is not expected to be strongly affected when shifting from the gas phase to the condensed one. ESIPT time constants as short as ~ 100 fs have been measured in liquids as well as in rigid polymeric media [65]. However, when the PES contains a barrier energy as reported here in HPPO and HAN, the solvent could affect the barrier as well as the energy gap (reaction free energy) between the enol and product forms. Solvation effect on excited dipoles is expected and has been reported in several cases [3,66]. The density of states for which the enol and tautomer forms are in resonance for the transfer depends on a manifold of product vibrational states that are Franck–Condon coupled to the reactant state, and statistical effects of the solvent could influence the vibronic coupling between both states. This will

lead to a different rate constant as the density of states is changed. In fact, HAN in solution does not show the normally Stokes shifted fluorescence band; only the emission assigned to the tautomer was observed, independent of the excitation wavelength.

Picosecond studies of IVR in isolated molecules as well as in their complexes with the solvent (clusters) showed that the main difference introduced by the solvent is the large decrease of the amount of excess energy needed for rapid energy distribution. This amount of energy needed for IVR to occur compared to the bare molecule was related to the increased density-of-states in the solvated molecules. In the intermolecular proton transfer systems, like α-naphthol $\cdot (NH_3)_n$ clusters, mass and energy transfer occur between solute and solvent. For the α-NpOH $\cdot$ NH_3, the binding energy (due to H-bond) is large and IVR could be observable without dissociating the complex. Studies of the energy and time-resolved emission of the 1:1 complex provides an opportunity to test the influence of intermolecular modes and solute–solvent interactions on IVR. This gives the most basic information on the proton-transfer mechanism of this system. With the help of these isolated gas phase and cluster studies and with the aid of molecular dynamics, it should be possible to examine microscopically the solvent role in condensed-phase, proton-transfer dynamics.

Note added. There are two recent noteworthy contributions to the dynamics of proton-transfer reactions which we would like to mention here. First, the elegant work by the Castleman group on the femtosecond dynamics of ammonia clusters and the novel phenomenon of coulomb explosion. [See the articles by the Castleman group in Femtosecond Chemistry, Vol. II, eds. J. Manz and L. Wöste (Weinheim, 1995) p. 449, and in this special issue, and references therein.] Second, the femtosecond dynamics of double proton transfer in 7-azaindole dimers has been reported [A. Douhal, S.K. Kim and A.H. Zewail, Nature 378 (1995) 260], and such studies open up a special direction of study in a novel class of systems. We are continuing such studies.

Acknowledgements

This work was supported by a grant from the National Science Foundation, the Universidad of Castilla-La Mancha (Spain) and by the project PB93-0126 (Spain). A.D. thanks Professor A.H. Zewail and the members of his group for their hospitalities during his stay at Caltech. We wish to thank Dr. Spencer Baskin for his help and for the careful reading of the manuscript.

References

[1] E.F. Caldin and V. Gold, in: Proton-transfer reactions (Chapmann and Hall, London, 1975).
[2] Faraday Discussions Chem. Soc. (1940) 36*; (1965) 39; (1982) 74.
[3] A. Douhal, J. Phys. Chem. 98 (1994) 13131, and references therein.
[4] A.B. Kotlyar, N. Borovok, S. Nachliel and M. Gutman, Biochem. 33 (1994) 873, and references therein.
[5] A. Weller, Elektrochemie 56 (1952) 662.
[6] A. Douhal, F. Amat-Guerri, M.P. Lillo and U.A. Acuna, J. Photochem. Photobiol. A 78 (1994) 127.
[7] A. Douhal, F. Amat-Guerri and A.U. Acuña, J. Phys. Chem. 99 (1995) 76.
[8] P.M. Felker, W.R. Lambert and A.H. Zewail, J. Chem. Phys. 77 (1982) 1603.
[9] T. Elsaesser and W. Kaiser, Chem. Phys. Letters 128 (1986) 231.
[10] S. Nagaoka and U. Nagashima, Chem. Phys. 136 (1989) 153.
[11] J. Catalan and J.I. Fernandez-Alonso, J. Mol. Struct. 27 (1975) 59; M. Sanchez-Cabezudo, J.L. De Paz, J. Catalan and F. Amat-Guerri, J. Mol. Struct. 131 (1985) 277; W.H. Orttung, G.W. Scott and D. Vosooghi, J. Mol. Struct. 109 (1985) 161.
[12] J. Goodman and L.E. Brus, J. Am. Chem. Soc. 100 (1978) 7472.
[13] A.L. Sobolewski and W. Domcke, Chem. Phys. 184 (1994) 115.
[14] M.V. Vener and S. Scheiner, J. Phys. Chem. 99 (1995) 642.
[15] A.U. Acuña, F. Amat-Guerri, J. Catalan and F. Gonzalez-Tablas, J. Phys. Chem. 84 (1980) 629.
[16] A.U. Acuña, J. Catalan and F. Toribio, 85 (1981) 241.
[17] J. Catalan, F. Toribio and A.U. Acuña, 86 (1982) 303; F. Toribio, J. Catalan, F. Amat-Guerri and A.U. Acuna, 87 (1983) 817; A.U. Acuna, F. Amat-Guerri, F. Toribio and J. Catalan, J. Photochem. 30 (1985) 330.
[18] P.F. Barbara, P.K. Walsh and L.E. Brus, J. Phys. Chem. 93 (1989) 29.
[19] J.L. Herek, S. Pedersen, L. Bañares and A.H. Zewail, J. Chem. Phys. 97 (1992) 9046.
[20] A. Douhal, F. Lahmani and A. Zehnacker-Rentien, Chem. Phys. 178 (1993) 493.
[21] A. Douhal, F. Lahmani, A. Zehnacker-Rentien and F. Amat-Guerri, J. Phys. Chem. 98 (1994) 12198.
[22] S.J. Formosinho and L. Arnaut, J. Photochem. Photobiol. A 75 (1993) 1, 21; S.W. Ormson and R.G. Brown, in: Progress

in reaction kinetics 1 (1994) 45; D. Le Gourrierec, S.W. Ormson and R.G. Brown, in: Progress in reaction kinetics 3 (1994) 211, and references therein.
[23] A. H. Zewail, Femtochemistry – ultrafast dynamics of the chemical bond (World Scientific, Singapore, 1994), and references therein.
[24] T. Elsaesser, in: Femtosecond chemistry, eds. J. Manz and L. Woste (VCH Verlag, Weinheim 1994).
[25] T. Arthen-Engeland, T. Bultmann, N.P. Ernsting, M.A. Rodriguez and W. Thiel, Chem. Phys. 163 (1992) 43.
[26] A. Muhlpfordt, T. Bultmann, N.P. Ernsting and B. Dick, in: Femtosecond reaction dynamics, ed. D.A. Wiersma (Royal Netherlands Academy of Arts and Sciences, Amsterdam, 1994) p. 83, and references therein.
[27] B.J. Schwartz, L.A. Peteanu and C.B. Harris, J. Phys. Chem. 96 (1992) 3591.
[28] A.H. Zewail, in: The chemical bond: structure and dynamics, ed. A.H. Zewail (Academic Press, Harcourt Brace Jovanovich, San Diego, 1992).
[29] A.H. Zewail, Faraday Discussions Chem. Soc. 91 (1991) 207.
[30] A.H. Zewail, in: Femtosecond chemistry, eds. J. Manz and L. Woste (VCH Verlag, Weinheim, 1994).
[31] P.O. Lowdin, Advan. Quantum Chem. 2 (1965) 213; R.P. Bell, The tunnel effect in chemistry (Chapmann and Hall, New York, 1980) ch. 2.
[32] T. Carrington and W.H. Miller, J. Chem. Phys. 84 (1986) 4364.
[33] M.F. Hineman, G.A. Brucker, D.F. Kelley and E.R. Bernstein, J. Chem. Phys. 97 (1992) 3341.
[34] J.A. Syage, J. Phys. Chem. 99 (1995) 5772.
[35] S.K. Kim, J.J. Breen, D.M. Willberg, L.W. Peng, A. Heikal, J.A. Syage and A.H. Zewail, J. Phys. Chem. 99 (1995) 7421.
[36] J.A. Syage, Faraday Discussions Chem. Soc. 97 (1994) 401.
[37] M. Dohle, J. Manz and G. K. Paramonov, Ber. Bunsenges. Physik. Chem. 99 (1995) 478.
[38] K.K. Smith and K. J. Kaufmann, J. Phys. Chem. 85 (1981) 2895, and references therein.
[39] L. Helmbrook, J.E. Kenny, B.E. Kohler and G.W. Scott, J. Chem. Phys. 75 (1981) 5201; J. Phys. Chem. 87 (1983) 280.
[40] T. Nishiya, S. Yamauchi, N. Hirota, M. Baba and I. Hanazaki, J. Phys. Chem. 90 (1986) 5730.
[41] S. Nagaoka, N. Hirota, M. Sumitani, K. Yoshihara, E. Lipczynska-Kochany and H. Iwanura, J. Am. Chem. Soc. 106 (1984) 6913; S. Nagaoka and U. Nagashima, J. Phys. Chem. 95 (1991) 4006.
[42] E. Orton, M.A. Morgan and G.C. Pimentel, J. Phys. Chem. 94 (1990) 7936.
[43] U. Shubert, E. Riedle, H.J. Neusser and E.W. Schlag, J. Chem. Phys. 84 (1986) 6182.
[44] P. Schuster, ed., Hydrogen bonds (Springer, Berlin, 1984).
[45] A. Douhal, F. Amat-Guerri, A.U. Acuña and K. Yoshihara, Chem. Phys. Letters 217 (1994) 619.
[46] C. Chudoba, S. Lutgen, T. Jentzsch, E. Riedle, M. Woerner and T. Elsaesser, Chem. Phys. Letters 240 (1995) 35.
[47] F. Lahmani, T. Ebata and A. Zehnacker-Rentien, unpublished results.
[48] G.J. Wolfe, M. Melzig, S. Schneider and F. Dorr, Chem. Phys. 77 (1983) 213.
[49] K. Ding, S.J. Courtney, A.J. Strandjord, S. Flom, D. Friedrich and P.F. Barbara, J. Phys. Chem. 87 (1983) 1184.
[50] A. Mordzinsky and K.H. Grellmann, J. Phys. Chem. 90 (1986) 5503.
[51] B. Nickel and A.A. Ruth, Chem. Phys. 184 (1994) 261, and references therein.
[52] W. Siebrand, T.A. Wildman and M.Z. Zgierski, J. Am. Chem. Soc. 106 (1984) 4083.
[53] E.A. Mangle, P.R. Salvi, R.J. Rabbit, A.L. Motika and M.R. Topp, Chem. Phys. Letters 133 (1987) 214.
[54] A. Ito, Y. Fujiwara and M. Itoh, J. Chem. Phys. 96 (1992) 7474, and references therein.
[55] M. Moreno et al., to be published.
[56] D. Huppert, E. Pines and N. Agmon, J. Opt. Soc. Am. B 7 (1990) 1545.
[57] E. Pines and G.R. Fleming, Chem. Phys. 183 (1994) 393.
[58] S.K. Kim, J.-K. Wang and A.H. Zewail, Chem. Phys. Letters 228 (1994) 369.
[59] L.L. Connell, Ph.D. Thesis, University of California, Los Angeles (1992).
[60] O. Cheshnovsky and S. Leutwyler, J. Chem. Phys. 88 (1988) 4127; 91 (1989) 1269.
[61] N. Mikami, A. Okabe and I. Suzuki, J, Phys. Chem. 92 (1988) 1858; S.T. Ceyer, P.W. Tiedeman, B.H. Mahan and Y.T. Lee, J. Chem. Phys. 70 (1979) 14.
[62] K. Ando and J.T. Hynes, ACS Symposium Series 568 (1994) 143.
[63] K.C. Ingham and M.A. Elbayoumi, J. Am. Chem. Soc. 96 (1974) 1682, and references therein.
[64] A. Douhal and R. Sastre, Chem. Phys. Letters 219 (1994) 91, and references therein.
[65] G.R. Fleming and P. Hanggi, eds., Activated barrier crossing (World Scientific, Singapore, 1993), and references therein.
[66] M. Wicchmann, H. Port, W. Frey, F. Laermer and T. Elsaesser, J. Phys. Chem. 95 (1991) 1918.